Combustion and Flame 266 (2024) 113543

Contents lists available at ScienceDirect

Combustion and Flame

journal homepage: www.sciencedirect.com/journal/combustion-and-flame

High-pressure oxidation of hydrogen diluted in N_2 with added H_2O or CO_2 at 100 atm in a supercritical-pressure jet-stirred reactor

Hao Zhao [a,b,*], Chao Yan [a], Guohui Song [a], Ziyu Wang [a], Ahren W. Jasper [c], Stephen J. Klippenstein [c], Yiguang Ju [a,*]

[a] Department of Mechanical and Aerospace Engineering, Princeton University, Princeton, NJ 08544, USA
[b] College of Engineering, Peking University, Beijing 100871, China
[c] Chemical Sciences and Engineering Division, Argonne National Laboratory, Lemont, IL 60439, USA

ARTICLE INFO

Keywords:
Supercritical kinetics
Hydrogen
Jet-stirred reactor
Ultra-high pressure
Real-fluid

ABSTRACT

The oxidation of H_2 diluted in N_2 with and without 10 % H_2O or 20 % CO_2 additions are studied at fuel-lean conditions at 100 atm and 500–1000 K in a supercritical-pressure jet-stirred reactor. The mole fractions of H_2 and O_2 are quantified by using micro-gas chromatography (μ-GC). Experiment shows that H_2 oxidation is inhibited at lower temperatures (850–950 K) while it is promoted at higher temperatures (950–1050 K) with 10 % H_2O additions or 20 % CO_2 additions. In addition, the effect of H_2O is more significant than that of CO_2. Five models are employed in simulations of the observables. Unfortunately, all of these models fail to capture the effect of H_2O and CO_2 additions on H_2 oxidation. Pathway and sensitivity analyses of H_2 show that the reactions of $H + O_2 + (M) = HO_2 + (M)$ and $H_2O_2 + (M) = 2OH + (M)$ dominate the radical production (HO_2 and OH) and H_2 oxidation at 100 atm. A further perturbation of pre-exponential coefficients and collisional factors of these reactions indicates that collisional factors of H_2O and CO_2 have small effect under the experimental conditions, while a smaller reaction rate for $H_2O_2 + (M) = 2OH + (M)$ may explain the inhibiting effect of H_2O and CO_2 additions at lower temperatures. Real-fluid corrections on intermolecular interactions and mixing rules should be further investigated to explain the effect of H_2O and CO_2 additions.

1. Introduction

As around 80 % of global energy is obtained from combustion of fossil fuels, it is critical to adopt innovative combustion strategies of carbon-free renewable fuels, such as H_2, for a low carbon society [1]. Among the advanced combustion strategies [2,3], such as Homogeneous Charge Compression Ignition and Reactivity Controlled Compression Ignition, an "ideal" burning condition of fuel lean, low temperature, and high pressure are optimal for high thermodynamic efficiencies (50–60 %) and low emissions. The "ideal" condition above generally falls into supercritical combustion regime, where most reactants are burned at the supercritical state. Moreover, with H_2 as the simplest fuel, its kinetics plays a foundational role in the hierarchical development of models for larger hydrocarbons and oxygenated fuels. Therefore, a better understanding of supercritical combustion of H_2 is vital for both kinetic studies and advanced engine designs.

In the supercritical state, intermolecular attractions become significant, and non-ideal fluid behavior can have substantial effects on the reaction kinetics, as well as the thermodynamic and transport properties. For instance, at ultra-high pressures, multiple-body collisions can cause significant deviations from the isolated binary collision assumptions of most gas-phase kinetic models [4,5]. This results in unconventional pressure dependencies, and the collisional cross-section area may differ from the potential of interactions in real fluids. Notably, thermodynamic properties like the heat capacity for CO_2 and H_2O can exhibit a 50 % variance from ideal gas values above 200 atm [6]. Consequently, there is a critical need for kinetic experiments and theoretical computations at pressures exceeding 100 atm to explore the chemistry of supercritical combustion.

Unfortunately, only a few experimental apparatuses, such as a shock tube [7,8], a high-pressure laminar flow reactor [9–12], and a supercritical-pressure jet-stirred reactor (SP-JSR) [4,5,13,14], can be used to study supercritical reaction chemistry under combustion conditions. The SP-JSR recently developed by Zhao et al. [4] provides a new experimental platform for studying supercritical fuel chemistry over an especially wide range of pressure and temperature (10–200 atm,

* Corresponding authors at: Department of Mechanical and Aerospace Engineering, Princeton University, Princeton, NJ 08544, USA.
E-mail addresses: h.zhao@pku.edu.cn (H. Zhao), yju@princeton.edu (Y. Ju).

https://doi.org/10.1016/j.combustflame.2024.113543
Received 26 April 2024; Received in revised form 28 May 2024; Accepted 30 May 2024
Available online 8 June 2024

295–1200 K), with excellent temperature uniformity (+/-3 K), and with a residence time (0.1–1.0 s) directly relevant to practical internal combustion engines. We recently studied the low and intermediate temperature chemistries of propane [14], n-butane [4], dimethyl ether (DME) [5], and methanol [13] at 100 atm using the SP-JSR, and developed high-pressure kinetic models, respectively.

As to the high-pressure studies of H_2 oxidation chemistry, Hong et al. [15] updated the H_2/O_2 reaction mechanism by incorporating their recent reaction rate determinations in shock tubes, and they emphasized significant uncertainties in the reaction rate of H_2O_2 decomposition at high pressure and in the collisional efficiencies for colliders other than Ar and N_2. Therefore, these third-body reactions involved in H_2O and CO_2 as colliders could have large uncertainties at high pressures. Meanwhile, Burke et al. [16] developed a high-pressure hydrogen oxidation mechanism based on their flame speed measurements [17,18] and other combustion targets. Lei et al. [19] also studied the nonlinear multi-component collision of $HO_2 + M = H + O_2 + M$ under high pressures, highlighting an error of several times in traditional collisional factor computations. Shao et al. [8] updated the high-pressure kinetic model of H_2 by measuring the ignition delay time of H_2 / O_2 / CO_2 at 250 atm. Mueller [20], Li [21], Davis [22], Hong [15], Burke [16], Keromnes [23], and others have respectively developed detailed chemical reaction mechanisms for H_2 either based on quantum chemistry computations or elementary reaction rate measurements. However, key rate coefficients in different kinetic models retain significant uncertainties. For example, errors in the H_2 adiabatic flame speed predictions for existing models reach up to a factor of 4 between different models at elevated pressures [17].

Clearly high uncertainties in the H_2 chemistry remain at high pressures, especially at supercritical conditions. In this work, the supercritical oxidation chemistry of H_2 is studied with the SP-JSR under fuel lean conditions at 100 atm and 500–1000 K, which extends the available data to engine conditions. The mole fractions of H_2 and O_2 are quantified with a micro-gas chromatograph (μ-GC). Moreover, the effect of real-fluid H_2O and CO_2 on the H_2 oxidation is investigated by adding 10 % H_2O or 20 % CO_2 to the reactant mixture. Comparisons with simulations based on five representative models are made in the exploration of the H_2 oxidation chemistry under these conditions. The key high-pressure reactions are identified through reaction pathway and sensitivity analyses for H_2. Updates are made to the rate parameters for some of these key reactions on the basis of ab initio kinetics.

2. Experimental methods and kinetic models

H_2 oxidation experiments are performed in the SP-JSR system, as is shown in Fig. 1. The SP-JSR is a spherical bulb with an internal volume of 0.5 cm^3. It contains 4 fingers with 2 jets (0.2 mm I. D.) on each finger at the center of the bulb, which enables optimized jet orientations for intense turbulence mixing to improve the mixing and homogeneity of reactant and temperature distributions. The quartz reactor is placed inside a stainless-steel pressure-resistant jacket. The inside and outside pressures of the reactor are balanced by the bath gas flow to reach the high-pressure conditions. The gases issuing from the SP-JSR exit are sampled by a quartz sonic nozzle, and then equilibrate their pressure with vacuum around 10^{-2} Torr generated by a dry pump. The experimental system is designed for experiments over pressures of 10-200 atm and temperatures of 298–1200 K. Further details of the SP-JSR and its jet and heating arrangements are provided in the literature [4]. The gas flow rates are controlled by high-pressure mass flow controllers (Brooks, SLA5800). Liquid water was delivered by a high performance liquid chromatography (HPLC) pump to a home-made high-pressure pre-vaporizer. The vaporized water vapor was carried by N_2 to the oxidizer line. Gas samples are quantified by using a micro-gas chromatography-thermal conductivity detector (GC-TCD, Inficon 3000) within 5 % errors [24]. The axial temperature profiles under the experimental flow conditions are measured in 1 mm steps along the JSR bulb, where

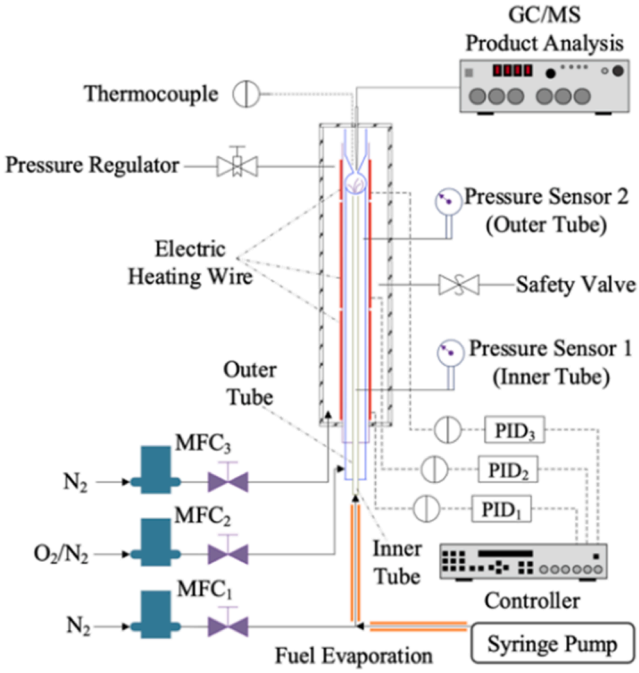

Fig. 1. Schematic of the SP-JSR setup.

the temperature variation is within ± 3 K between 500 and 1000 K. The details of the temperature profile measurement are provided in [5]. The repeated samples fall within the 5 % error for all conditions, which mainly comes from fuel purity and GC-TCD quantifications, while the temperature variations contribute to the measurement errors.

The experiment is performed at fuel lean conditions with and without H_2O and CO_2 additions at 100 atm between 500–1000 K, as is shown in Table 1. The residence time in the reactor varies with reactor temperature (T) to keep a fixed inlet volume flow rate at 4 L/min at 293 K through $\tau = (V / \upsilon) * T_0 / T$, where, V is the volume of the JSR, υ is the inlet volume flow rate at room temperature, T_0 is the room temperature (293 K). Simulations are performed in the PSR module of CHEMKIN software [25] by using five H_2 models, Aramco Mech 3.0 [26], Dagaut Mech [27], FFCM Mech [28], Hashemi Mech [10], and the updated HP Mech based on HP Mech [29] with including recently updated key elementary reaction rates for H_2 chemistry as summarized in Table 2. The present theoretical kinetic predictions for the reaction of H_2O_2 with H derive from earlier unpublished work of Wu et al. [30] through high-level quantum chemistry computations, which has been described in detail in the supplementary material. The third-body collision efficiencies of $H_2O_2 + (M) = 2OH + (M)$ were taken from previous calculations involving a combination of collisional energy transfer trajectories and master equation analyses [31,32]. In particulate, an average value of 8.71 was picked for the third-body efficiency of H_2O.

3. Results and discussion

The experimental and modeling results for oxidation of H_2 diluted in N_2 at 100 atm are plotted in Fig. 2. Most models, such as Aramco Mech 3.0, Dagaut Mech, FFCM Mech, Hashemi Mech, and updated HP Mech predict H_2 and O_2 mole fractions that agree reasonably well with the experimental measurements, exhibiting accurate predictions of the H_2 oxidation in N_2 dilutions at 100 atm.

Fig. 3 (a) and (b) depict the H_2 evolution against temperature with 10 % H_2O additions and 20 % CO_2 additions, respectively, at 100 atm. In Fig. 3 (a), the onset temperature of the H_2 oxidation with 10 % H_2O additions is delayed, resulting in a right shift of the oxidation scatter between 850 and 950 K. However, at higher temperatures, the H_2

Table 1
Experimental conditions.

Case	Equivalence ratio	Pressure (atm)	H_2 (%)	O_2 (%)	N_2 (%)	CO_2 (%)	H_2O (%)	Residence time (s)	Temperature (K)
1	0.343	100	3.248	4.738	92.014	0	0	0.352-0.195	500-1000
2	0.343	100	3.248	4.738	82.014	0	10.000	0.352-0.195	500-1000
3	0.343	100	3.248	4.738	72.090	19.924	0	0.352-0.195	500-1000

Table 2
Updated reaction rates in updated HP Mech from the HP base Mech.

Reactions	A (cm^3 /$mol.s$)	n	Ea (cal /mol)	Refs.
$H_2O_2 + H = H_2O + OH$	3.35E+07	1.91	3654	Present
$H_2O_2+H=H_2+HO_2$	44.00E+00	3.45	712	Present
H_2O_2 (+M) = 2OH (+M)	2.00E+12	0.9	48749	[31,
LOW	2.49E+24	-2.3	48749	32]
TROE	0.43	1.0E-30	1.0E+30	
H_2O/8.71/ CO_2/4.79/ N_2/ 2.07/ O_2/1.5/ He/1.00/ H_2O_2/8.07/ H_2/3.7/ CO/2.8/				
$HO_2 + HO_2 = H_2O_2 + O_2$	1.93E-02	4.12	-4960	[33]
$HO_2 + HO_2 = OH + OH + O_2$	6.41E+17	-1.54	8540	[33]

oxidation with H_2O additions is promoted, leading to a left shift of the scatter between 950 and 1050 K. Therefore, H_2O additions "twist" the H_2 oxidation more steeply. In Fig. 3 (b), 20 % CO_2 additions show a similar effect on H_2 oxidation as the 10 % H_2O addition of case 2 did, although its impact is somewhat smaller than for the only 10 % H_2O additions. That reduction is likely because H_2O is a highly polar molecule and exhibits a stronger intermolecular interaction than CO_2 at high pressures. As to model predictions, unfortunately, all of the five models exhibit little difference from the purely N_2 diluted case for both H_2O or CO_2 additions. They clearly fail to capture the experimentally observed effect of H_2O and CO_2 additions on H_2 oxidation.

The mole fraction of O_2 at 100 atm for 10 % H_2O addition and 20 % CO_2 addition are plotted in Fig. 4 (a) and (b), respectively. In the experiments, H_2O and CO_2 additions delay the consumption of O_2 at lower temperatures, but accelerate it at higher temperature, which agree with

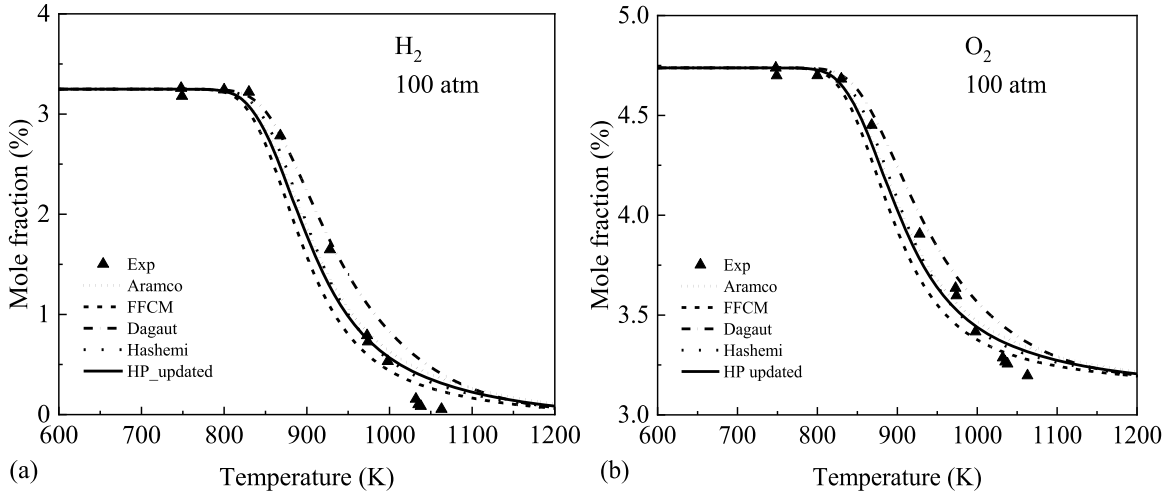

Fig. 2. Mole fractions of H_2 and O_2 in the oxidation of H_2 diluted in N_2 at 100 atm.

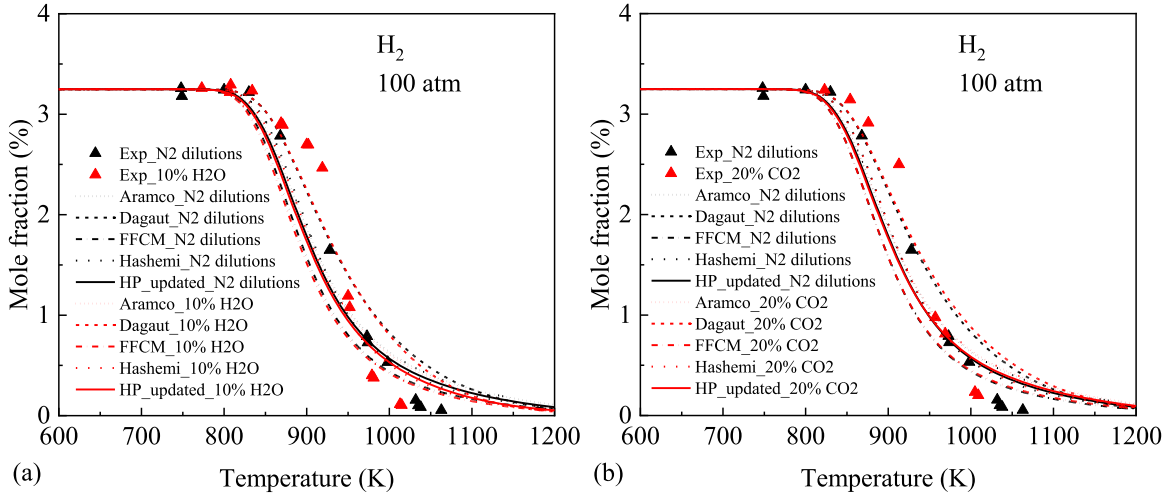

Fig. 3. Mole fraction of H_2 in H_2 oxidation with 10 % H_2O additions (a) and 20 % CO_2 additions (b) at 100 atm.

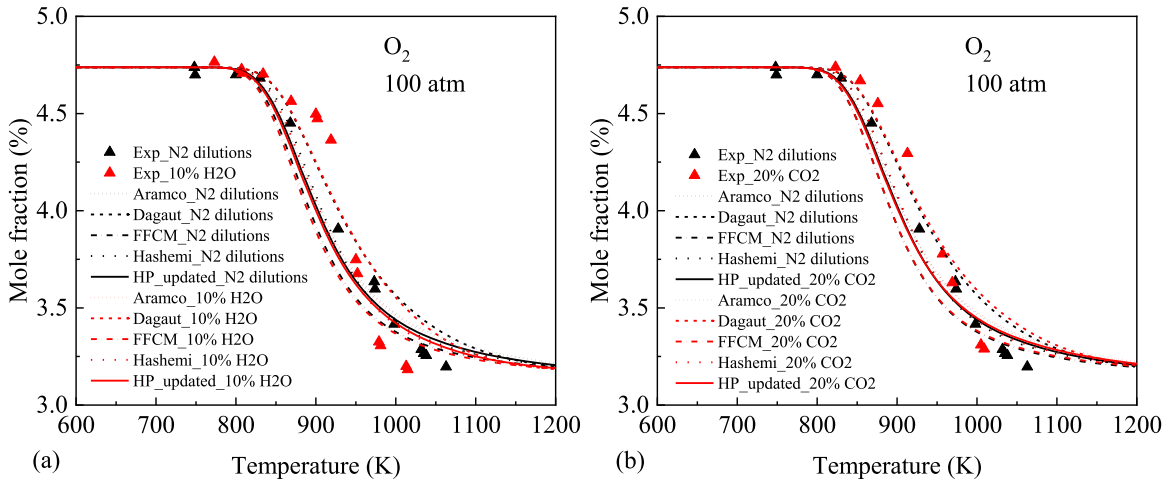

Fig. 4. Mole fraction of O_2 in H_2 oxidation in 10 % H_2O additions (a) and 20 % CO_2 additions (b) at 100 atm.

the observations in Fig. 3. Similarly, H_2O and CO_2 additions in the simulations show little impact on O_2 oxidation compared to the case for pure N_2 dilution.

To explain the key characteristics in H_2 oxidation, the pathway analyses of H_2 in N_2 dilution, with 10 % H_2O, and with 20 % CO_2 are plotted in Fig. 5 (a–c), respectively, at 875 K and 100 atm by using updated HP Mech. In Fig. 5 (a), the H abstraction reaction of OH + H_2 dominates the H_2 oxidation pathway and produces H_2O and H. The H radical combines with O_2 and forms HO_2 very rapidly through the third-body reaction H + O_2 + (M) = HO_2 + (M). Then, H_2O_2, formed from HO_2, produces two OH radicals through H_2O_2 + (M) = 2OH + (M). Moreover, it is well known that H + O_2 = OH + O is a crucial branching reaction competing with H + O_2 + (M) = HO_2 + (M) at low pressures or high temperatures. However, the radical production from H + O_2 = OH + O almost disappears at 100 atm. Thanks to the high pressure, the third-body reaction H + O_2 + (M) = HO_2 + (M) is enhanced dramatically and dominates the radical production and O_2 consumption pathways. The discussion above agrees with the typical 3rd explosion limit of H_2. The kinetic effect of H_2O or CO_2 additions on H_2 oxidation is mainly through altering the reaction rates of the third-body reactions, such as H + O_2 + (M) = HO_2 + (M) and H_2O_2 + (M) = 2OH + (M). Unfortunately, the production fluxes of H + O_2 + (M) = HO_2 + (M) and H_2O_2 + (M) = 2OH + (M) in Fig. 5(b) and (c) show little differences from that in Fig. 5 (a). In addition, H_2O_2 formation in these three cases is manly from HO_2+HO_2 reactions, which accounts for 73.3 % of the H_2O_2 production flux, while a minor reaction path is HO_2+H_2.

To identify key reactions in H_2 oxidation, the sensitivity analyses of H_2 diluted in N_2, with 10 % H_2O, and with 20 % CO_2 are plotted in Fig. 6 (a–c), respectively, at 875K and 100 atm by using updated HP Mech. In Fig. 6(a), it is seen that reactions involved in H_2O_2 pathways are most sensitive, such as HO_2 + HO_2 = H_2O_2 + O_2 (duplicated reactions in updated HP Mech), H_2O_2 + (M) = 2OH + (M), and H_2O_2 + OH = HO_2 + H_2O. It indicates that H_2 oxidation at high pressure is controlled by HO_2 and H_2O_2 chemistry, which explains the broadly enhanced warm flame chemistry in our previous oxidation studies of propane, dimethyl ether, and n-butane at 100 atm [4,5,14]. Similarly, Fig. 6 (b) and (c) shows little difference in the sensitive reactions from Fig. 6(a).

It is noted that the reactions H + O_2 + (M) = HO_2 + (M) and H + O_2 = O + OH are less sensitive than the reactions above. Their reasons are different. The former is because its reaction rate becomes dramatically fast at high pressures and is close to the partial equilibrium assumption, while the latter is relatively much slower than the former, leading to a "frozen" reaction even at high temperatures. This argument also agrees with the pathway analysis in Fig. 5. Therefore, reactions involved with OH become very important as OH is mainly produced from H_2O_2 + (M) = 2OH + (M) at high pressures, such as H_2 + OH = H + H_2O; while reactions with O are frozen as O is mainly produced from H + O_2 = O + OH, such as O + H_2 = OH + H. In addition, compared with Fig. 6(a), reactions H_2 + OH = H + H_2O and HO_2 + OH = O_2 + H_2O become more sensitive with H_2O or CO_2 additions in Fig. 6(b) and (c). That is because the average collisional factor of the mixture increases with H_2O or CO_2 additions and enhances the OH concentrations from H_2O_2 + (M) = 2OH + (M). H_2O_2 + H = H_2 + HO_2 also becomes sensitive with CO_2 addition as the reaction CO + OH = H + CO_2 is suppressed with CO_2 addition.

Several possible reasons are proposed here to explain the effects of H_2O and CO_2 addition on H_2 oxidations: (i) pre-exponential coefficients of H + O_2 + (M) = HO_2 + (M) and H_2O_2 + (M) = 2OH + (M); (ii) collisional factor (M factor) of the reactions above; (iii) real-fluid corrections on reaction rate calculations.

Therefore, the perturbations of pre-exponential coefficients and collisional factors of H + O_2 + (M) = HO_2 + (M) and H_2O_2 + (M) = 2OH + (M) on H_2 oxidation are investigated in Fig. 7(a) and (b), respectively,

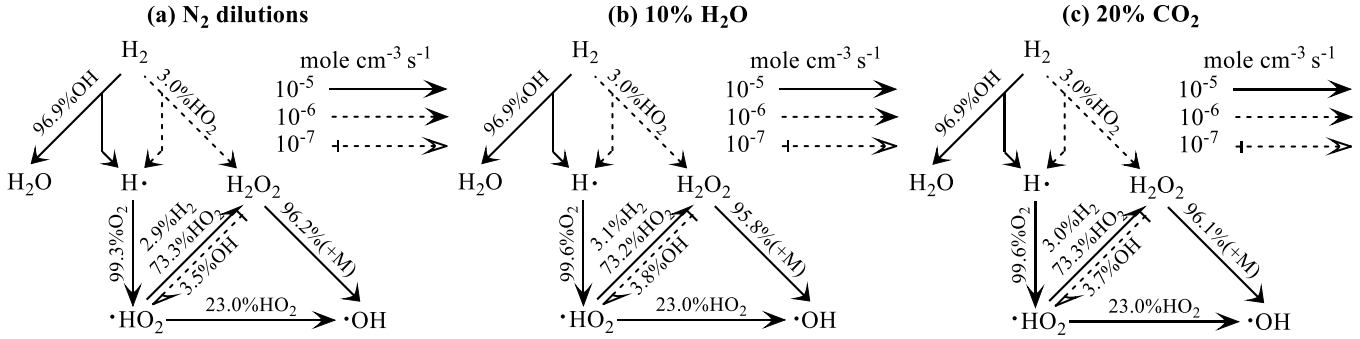

Fig. 5. Reaction pathways for H_2 diluted in N_2 (a), with 10 % H_2O addition (b), and with 20 % CO_2 addition (c) at 875 K and 100 atm by using updated HP Mech.

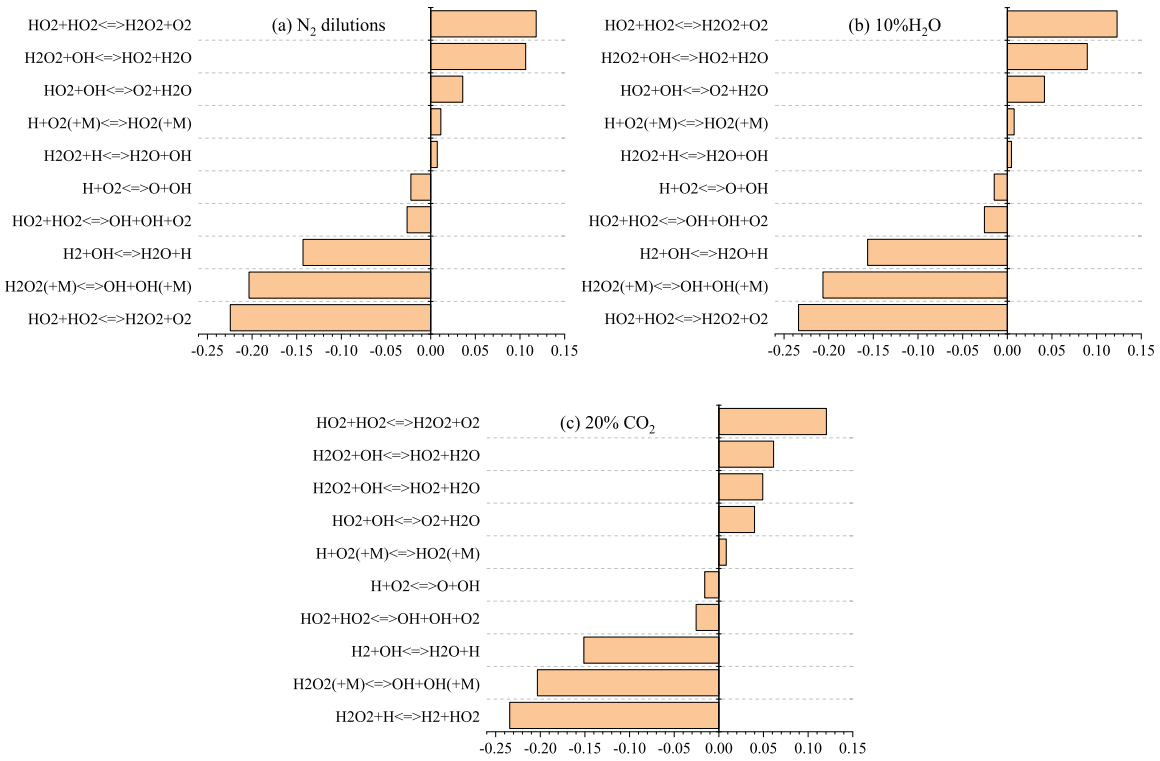

Fig. 6. Sensitivity analyses for H_2 diluted in N_2 (a), with 10 % H_2O addition (b), and with 20 % CO_2 addition (c) at 875 K and 100 atm by using updated HP Mech.

at 100 atm by using updated HP Mech. In Fig. 7(a), compared with oxidation of H_2 diluted in N_2, addition of H_2O exhibits little impact on the oxidation in the modelling. By reducing the pre-exponential coefficient of $H_2O_2 + (M) = 2OH + (M)$ in the high-pressure limit expression of a Troe format by a factor of 0.1, the oxidation is significantly delayed, while increasing the reaction rate of $H + O_2 + (M) = HO_2 + (M)$ by a factor of 100 has little impact. This finding agrees with the discussion of the two reactions above in the sensitivity analysis. Therefore, it looks like a smaller rate of $H_2O_2 + (M) = 2OH + (M)$ in simulations reduces the discrepancy with experiments.

In Fig. 7(b), we further perturb H_2 oxidation by altering the H_2O addition and the collisional factors of N_2 and H_2O for $H_2O_2 + (M) = 2OH + (M)$. It is seen that a 90 % addition of H_2O accelerates the oxidation significantly as the collisional factor of H_2O is ~4 times larger than N_2 as a major bath gas, while it fails to explain the inhibiting effect of H_2O addition on H_2 oxidation at lower temperatures in experiments. In the case of pure N_2 dilutions or with 10 % H_2O addition, the change of the collisional factor of N_2 plays a major role in affecting the rate of $H_2O_2+(M)$ as N_2 is the major bath gas. However, the change of the collisional factor of H_2O has no impact, even though the collisional factor of H_2O is reduced by 100 times. Therefore, we think the update of the collisional factor of H_2O in $H_2O_2 + (M) = 2OH + (M)$ from the current model could not explain the present experimental results.

According to the discussion above, a smaller reaction rate of $H_2O_2 + (M) = 2OH + (M)$ may explain the inhibiting effect of H_2O addition at lower temperatures. Other possible reasons, such as real-fluid

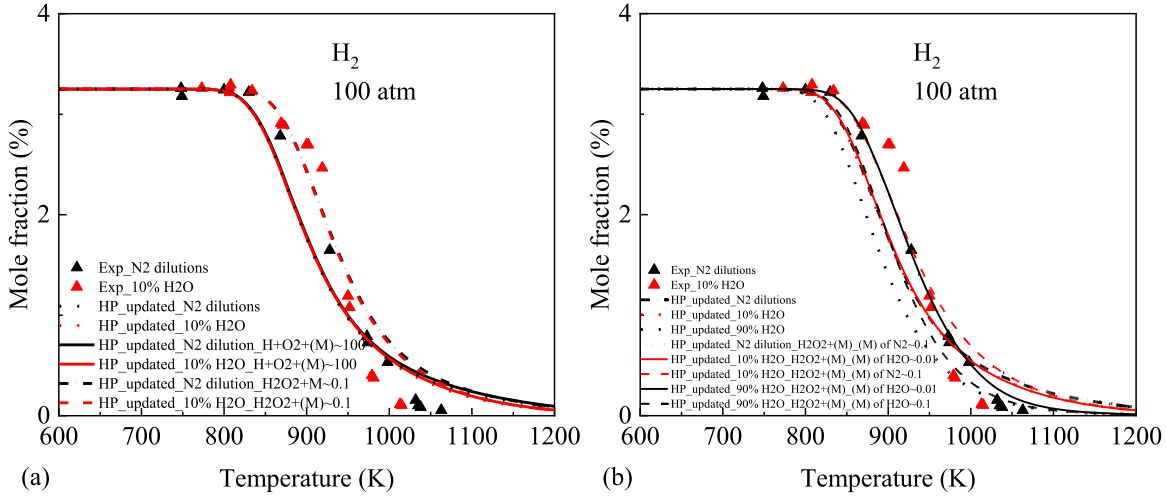

Fig. 7. (a) Effect of pre-exponential coefficients of $H + O_2 + (M) = HO_2 + (M)$ (increase by a factor of 100) and $H_2O_2 + (M) = 2OH + (M)$ (decrease by a factor of 0.1) on H_2 oxidation at 100 atm by using updated HP Mech; (b) Effect of different collisional factors (M factor) of N_2 and H_2O for $H_2O_2 + (M) = 2OH + (M)$ on H_2 oxidation at 100 atm by using updated HP Mech.

corrections to the intermolecular force field, collisional cross-sections, mixing rules, and multi-body collisions should be further investigated to explain the effect of H_2O and CO_2 additions.

4. Conclusion

The supercritical pressure jet stirred reactor provides a valuable platform for performing kinetic studies at low and intermediate temperatures at extreme pressures with a uniform temperature distribution and a short flow residence time. The oxidations of H_2 diluted in N_2, with 10 % H_2O, or 20 % CO_2 addition are studied at 100 atm and 500-1000 K in SP-JSR experiments. The mole fractions of H_2 and O_2 are quantified with a micro-gas chromatograph (μ-GC). Experiment shows that H_2 oxidation is inhibited at lower temperatures (850–950 K), while it is promoted at higher temperatures (950–1050 K) with 10 % H_2O addition or 20 % CO_2 addition. Simply put, H_2O or CO_2 additions "twist" the H_2 oxidation more steeply. In addition, the effect of H_2O is more significant than that of CO_2, while the reaction $H_2O_2 + H = H_2 + HO_2$ becomes more sensitive with CO_2 addition.

Five models (Aramco Mech 3.0, Dagaut Mech, FFCM Mech, Hashemi Mech, and updated HP Mech) are employed in the present simulations. Unfortunately, all of these models fail to capture the effect of H_2O and CO_2 additions on H_2 oxidation. Through the pathway analyses and sensitivity analyses of H_2, it is seen that the reactions of $H + O_2 + (M) = HO_2 + (M)$ and $H_2O_2 + (M) = 2OH + (M)$ dominate the radical production (HO_2 and OH) and H_2 oxidation at 100 atm.

A further perturbation of pre-exponential coefficients and collisional factors for the above reactions indicates that the change of their collisional factors has little effect on H_2 oxidation, while a smaller reaction rate of $H_2O_2 + (M) = 2OH + (M)$ may explain the inhibiting effect of H_2O and CO_2 additions at lower temperatures. Other possible reasons, such as real-fluid corrections on intermolecular force field, collisional cross-sections, mixing rules, and multi-body collisions should be further investigated to explain the effect of H_2O and CO_2 additions.

Novelty and significance statement

Supercritical combustion gains increasing attentions for its high thermodynamic efficiency and low emissions, and it is widely employed in advanced combustion engines and rockets. However, non-ideal fluid behaviors under supercritical conditions can have substantial effects on the reaction kinetics, and high uncertainties in the H_2 chemistry remain at high pressures with limited experimental data as well. The present work provides important speciation data in H_2 oxidation at 100 atm by using the first supercritical-pressure jet-stirred reactor, and develops a new H_2 model for supercritical combustion by updating several key elementary reactions. A special real-fluid impact of H_2O or CO_2 additions on H_2 oxidation has been revealed in experiments, while is not predicted in existing models. This work emphasizes the real-fluid corrections on intermolecular interactions and mixing rules for the community of supercritical combustion as future work.

CRediT authorship contribution statement

Hao Zhao: Writing – review & editing, Writing – original draft, Software, Methodology, Data curation, Conceptualization. **Chao Yan:** Writing – review & editing, Methodology, Data curation. **Guohui Song:** Formal analysis, Data curation. **Ziyu Wang:** Writing – review & editing, Software, Data curation. **Ahren W. Jasper:** Writing – review & editing, Software, Data curation. **Stephen J. Klippenstein:** Methodology, Writing – review & editing. **Yiguang Ju:** Writing – review & editing, Supervision, Funding acquisition.

Declaration of competing interest

The authors declare that they have no known competing financial interests or personal relationships that could have appeared to influence the work reported in this paper.

Acknowledgment

This work was supported by the DOE BES award DE-SC0021135, and the DOE BES award DE-AC02-06CH11357. Support for A.W.J. and S.J.K. was provided in part by the Consortium on Pressure-Dependent Chemistry, FWP# 2009 ANL 59044.

Supplementary materials

Supplementary material is submitted along with the manuscript. The updated HP Mech for H_2 is also included in the supplementary material.

Supplementary material associated with this article can be found, in the online version, at doi:10.1016/j.combustflame.2024.113543.

References

[1] S. Brynolf, M. Taljegard, M. Grahn, J. Hansson, Electrofuels for the transport sector: A review of production costs, Renew. Sustain. Energy Rev. 81 (2018) 1887–1905.
[2] M. Yao, Z. Zheng, H. Liu, Progress and recent trends in homogeneous charge compression ignition (HCCI) engines, Prog. Energy Combust. Sci. 35 (2009) 398–437.
[3] Y. Li, M. Jia, Y. Chang, Y.D. Liu, M.Z. Xie, T.Y. Wang, L. Zhou, Parametric study and optimization of a RCCI (reactivity controlled compression ignition) engine fueled with methanol and diesel, Energy 65 (2014) 319–332.
[4] H. Zhao, C. Yan, T. Zhang, G. Ma, M. Souza, C. Zhou, Y. Ju, Studies of high-pressure n-butane oxidation with CO_2 dilution up to 100 atm using a supercritical-pressure jet-stirred reactor, Proc. Combust. Inst. 38 (2021) 279–287.
[5] C. Yan, H. Zhao, Z. Wang, et al., Low- and intermediate-temperature oxidation of dimethyl ether up to 100 atm in a supercritical pressure jet-stirred reactor, Combust. Flame 243 (2022) 112059.
[6] J. Bai, P. Zhang, C.-W. Zhou, H. Zhao, Theoretical studies of real-fluid oxidation of hydrogen under supercritical conditions by using the Virial equation of state, Combust. Flame 243 (2022) 111945.
[7] G. Kogekar, C. Karakaya, G.J. Liskovich, M.A. Oehlschlaeger, S.C. DeCaluwe, R. J. Kee, Impact of non-ideal behavior on ignition delay and chemical kinetics in high-pressure shock tube reactors, Combust. Flame 189 (2018) 1–11.
[8] J. Shao, R. Choudhary, D.F. Davidson, R.K. Hanson, S. Atmak, S. Vasu, Ignition delay times of methane and hydrogen highly diluted in carbon dioxide at high pressures up to 300 atm, Proc. Combust. Inst. 37 (2019) 4555–4562.
[9] G. Li, Y. Lu, P. Glarborg, Development of a detailed kinetic model for hydrogen oxidation in supercritical H_2O/CO_2 mixtures, Energy Fuels 34 (2020) 15379–15388.
[10] H. Hashemi, J.M. Christensen, S. Gersen, H. Levinsky, S.J. Klippenstein, P. Glarborg, High-pressure oxidation of methane, Combust. Flame 172 (2016) 349–364.
[11] H. Hashemi, J.G. Jacobsen, C.T. Rasmussen, J.M. Christensen, P. Glarborg, S. Gersen, M. van Essen, H.B. Levinsky, S.J. Klippenstein, High-pressure oxidation of ethane, Combust. Flame 182 (2017) 150–166.
[12] H. Hashemi, J.M. Christensen, L.B. Harding, S.J. Klippenstein, P. Glarborg, High-pressure oxidation of propane, Proc. Combust. Inst. 37 (2019) 461–468.
[13] Z. Wang, H. Zhao, C. Yan, et al., Methanol oxidation up to 100 atm in a supercritical pressure jet-stirred reactor, Proc. Combust. Inst. 39 (2023) 445–453.
[14] H. Zhao, C. Yan, G. Song, Z. Wang, Y. Ju, Studies of low and intermediate temperature oxidation of propane up to 100 atm in a supercritical-pressure jet-stirred reactor, Proc. Combust. Inst. 39 (2023) 2715–2723.
[15] Z. Hong, D.F. Davidson, R.K. Hanson, An improved H_2/O_2 mechanism based on recent shock tube/laser absorption measurements, Combust. Flame 158 (2011) 633–644.
[16] M.P. Burke, M. Chaos, Y. Ju, et al., Comprehensive H_2/O_2 kinetic model for high-pressure combustion, Int. J. Chem. Kinet. 44 (2012) 444–474.
[17] M.P. Burke, M. Chaos, F.L. Dryer, Y. Ju, Negative pressure dependence of mass burning rates of $H_2/CO/O_2$/diluent flames at low flame temperatures, Combust. Flame 157 (2010) 618–631.
[18] M.P. Burke, F.L. Dryer, Y. Ju, Assessment of kinetic modeling for lean $H_2/CH_4/O_2$/diluent flames at high pressures, Proc. Combust. Inst. 33 (2011) 905–912.
[19] L. Lei, M.P. Burke, Mixture rules and falloff are now major uncertainties in experimentally derived rate parameters for $H + O_2 (+M) \leftrightarrow HO_2 (+M)$, Combust. Flame 213 (2020) 467–474.
[20] M.A. Mueller, T.J. Kim, R.A. Yetter, F.L. Dryer, Flow reactor studies and kinetic modeling of the H_2/O_2 reaction, Int. J. Chem. Kinet. 31 (2) (1999) 113–125.
[21] J. Li, Z. Zhao, A. Kazakov, F.L. Dryer, An updated comprehensive kinetic model of hydrogen combustion, Int. J. Chem. Kinet. 36 (2004) 566–575.
[22] S.G. Davis, A.V. Joshi, H. Wang, F. Egolfopoulos, An optimized kinetic model of H_2/CO combustion, Proc. Combust. Inst. 30 (2005) 1283–1292.
[23] A. Keromnes, W.K. Metcalfe, K.A. Heufer, et al., An experimental and detailed chemical kinetic modelling study of hydrogen and syngas mixtures at elevated pressures, Combust. Flame 160 (2013) 995–1011.

[24] H. Zhao, L. Wu, C. Patrick, Z. Zhang, Y. Rezgui, X. Yang, G. Wysocki, Y. Ju, Studies of low temperature oxidation of n-pentane with nitric oxide addition in a jet stirred reactor, Combust. Flame 197 (2018) 78–87.
[25] CHEMKIN-PRO, (2011). http://www.reactiondesign.com/products/.
[26] X. Zhang, J. Zou, C. Cao, W. Chen, J. Yang, F. Qi, Y. Li, Exploring the low-temperature oxidation chemistry of 1-butene and i-butene triggered by dimethyl ether, Proc. Combust. Inst. 38 (2021) 289–298.
[27] T.L. Cong, P. Dagaut, Oxidation of H_2/CO_2 mixtures and effect of hydrogen initial concentration on the combustion of CH_4 and CH_4/CO_2 mixtures: Experiments and modeling, Proc. Combust. Inst. 32 (2009) 427–435.
[28] G.P. Smith, Y. Tao, H. Wang. Foundational Fuel Chemistry Model, 2016, Version 1.0 (FFCM-1),. http://nanoenergy.stanford.edu/ffcm1.
[29] H. Zhao, J. Fu, F.M. Haas, Y. Ju, Effect of prompt dissociation of formyl radical on 1, 3, 5-trioxane and CH_2O laminar flame speeds with CO_2 dilution at elevated pressure, Combust. Flame 183 (2017) 253–260.
[30] C.-H. Wu, W.D. Allen, S.J. Klippenstein, unpublished, (2011).
[31] A.W. Jasper, Predicting third-body collision efficiencies for water and other polyatomic baths, Faraday Discuss. 238 (2022) 68–86.
[32] D.R. Moberg, A.W. Jasper, Permutationally invariant polynomial expansions with unrestricted complexity, J. Chem. Theory Comput. 17 (2021) 5440–5455.
[33] S.J. Klippenstein, R. Sivaramakrishnan, U. Burke, et al., $HO_2 + HO_2$: High level theory and the role of singlet channels, Combust. Flame 243 (2022) 111975.